JB Accepts, published online ahead of print on 21 December 2007
J. Bacteriol. doi:10.1128/JB.01469-07

Glycerate 2-kinase of Thermotoga maritima and genomic reconstruction of related metabolic pathways.

Chen Yang[‡§*], Dmitry A. Rodionov[‡¶*], Irina A. Rodionova[‡], Xiaoqing Li[‡], and Andrei L. Osterman[‡‖1]

From the [‡]Burnham Institute for Medical Research, La Jolla, California 92037, [§]Institute of Plant Physiology and Ecology, Shanghai Institutes for Biological Sciences, Chinese Academy of Sciences, Shanghai 200032, China, [¶]Institute for Information Transmission Problems, Russian Academy of Sciences, Moscow 127994, Russia, [‖]Fellowship for Interpretation of Genomes, Burr Ridge, Illinois 60527.

Running Title: Glycerate kinases in bacteria

* C.Y. and D.A.R contributed equally to this work.

[1]To whom correspondence should be addressed: Mailing address: Burnham Institute for Medical Research. 10901 North Torrey Pines Road, La Jolla, CA 92037. Phone: (858) 646-3100. Fax: (858) 795-5249. E-mail: osterman@burnham.org

Summary

Members of a novel Glycerate-2-kinase family (GK-II) were tentatively identified in a broad range of species, including eukaryotes, archaea, and many bacteria that lack a canonical enzyme of the GarK family (GK-I). A recently reported 3D structure of GK-II from *Thermotoga maritima* (TM1585, 2b8n) revealed a new fold distinct from other known kinase families. Here we verified the enzymatic activity of TM1585, assessed its kinetic characteristics, and used directed mutagenesis to confirm the essential role of the two active site residues Lys-47 and Arg-325. The main objective of this study was to apply comparative genomics for the reconstruction of metabolic pathways associated with GK-II in all bacteria, and in particular in *T. maritima*. Comparative analysis of ~400 bacterial genomes revealed a remarkable variety of pathways that lead to GK-II-driven utilization of glycerate via a glycolysis/gluconeogenesis route. In the case of *T. maritima*, a three-step serine degradation pathway was inferred based on tentative identification of two additional enzymes, serine-pyruvate aminotransferase and hydroxypyruvate reductase (TM1400 and TM1401, respectively) that convert serine to glycerate via hydroxypyruvate. Both enzymatic activities were experimentally verified, and the entire pathway was validated by its *in vitro* reconstitution.

Keywords: glycerate kinase; hydroxypyruvate reductase; serine aminotransferase; comparative genomics; metabolic reconstruction.

INTRODUCTION

Phosphorylation of glycerate by glycerate kinase (GK) is a key biochemical step connecting this important carbohydrate (a C_3-sugar acid) with central carbon metabolism in a large variety of species. A diversity of pathways supplying glycerate—including L-serine degradation, utilization of glyoxylate, glycolate, D-glucarate, and tartrate (see Fig. 1B)—in different species is matched by the emerging diversity of GK enzymes. GK can convert glycerate to 3-phosphoglycerate (3PG; EC 2.7.1.31) or to 2-phosphoglycerate (2PG; EC 2.7.1.-). So far at least three distinct GK families (GK-I, -II, and –III) with different phylogenetic distribution, which are classified based on the amino acid sequence and structure similarity, have been described (1, 2).

Members of the historically first GK family (termed here GK-I) are represented by two paralogous genes, *glxK* and *garK* of *E. coli*, involved in glyoxylate and glucarate/galactarate utilization pathways, respectively (5, 6, 18). GK-I family members that occur in many diverse bacteria are usually annotated as 3PG-forming enzymes based on the original report of Doughty et al. (6). However, more recent studies of GarK activity by ^{1}H NMR revealed the formation of 2PG rather than 3PG product (12). Notwithstanding the importance of an accurate assignment of GK-I family reaction specificity, it does not affect the interpretation of its physiological role, as 2PG and 3PG are readily interconverted by a phosphoglycerate mutase (PGM). The 3D structure of the GK-I enzyme from *Neisseria meningitides* was solved (PDB code 1to6) and classified as a separate structural family (2).

The first representative of a structurally distinct GK-II family was characterized in *Hypomicrobium methylovorum* (33) as an enzyme involved in serine cycle pathway coupled to formaldehyde assimilation. A gene *gckA* was later identified in another

methylotrophic bacterium, *Methylobacterium extorquens* (3). GK-II orthologs are found in many bacterial, eukaryotic, and archaeal genomes. A GK-II enzyme was characterized and shown to play an important role in serine degradation pathway in mammalian liver (15). A deficiency of human GK-II activity leads to the hereditary disease D-glyceric aciduria (31), which was tentatively connected with alternative splicing of the gene GLYCTK (9). Recently, a GK-II family member from the archaeon *Picrophilus torridus* (gene *gck*) was characterized as a key enzyme in the non-phosphorylating Entner-Doudoroff (NP-ED) pathway characteristic of thermoacidophilic archaea such as *P. torridus* and *Thermoplasma acidophilum* (24, 25). A recently reported first 3D structure of a GK-II family protein TM1585 from *T. maritima* (PDB code 2b8n) revealed a novel fold and allowed to tentatively map active site area (2, 29). Two characterized members of the GK-II family from *M. extorquens* (3) and *P. torridus* (24) were assigned 2PG-forming activity.

The third, structurally unrelated, GK family (termed here GK-III and also known as GLYK) includes the recently characterized 3PG-forming enzyme from *Arabidopsis thaliana* (1), and its homologs in other plants, fungi, nearly all cyanobacteria, and a few other bacterial species. In plants, GK-III catalyzes the final reaction of the photorespiratory cycle, which converts glycolate-2P to 3PG (1).

Of the three GK families, GK-II, while being less abundant in the current collection of bacterial genomes than GK-I, is the most universal one, spanning all three domains of life. However, until recently, functional assignments within this family remained somewhat controversial. Despite convincing genetic data first ascribing the GK function to GckA protein in the methylotrophic bacterium *M. extorquens* (3), other representatives of the GK-II family in many bacterial genomes were tentatively assigned a seemingly

unrelated function, *hydroxypyruvate reductase*, in various public archives such as NCBI, KEGG (see Results for our interpretation of this misannotation). The main objective of this study was to apply comparative genomics for the reconstruction of metabolic pathways associated with GK-II in a broad range of bacterial species with completely sequenced genomes integrated in the SEED platform (http://theseed.uchicago.edu, (22)). This analysis captured in the SEED subsystem "Glycerate metabolism" (see http://theseed.uchicago.edu/FIG/subsys.cgi and Supplementary Table S1) allowed us to infer functional context (metabolic pathways) of the GK-II family in >60 bacterial genomes.

In the case study of *T. maritima*, we performed the experimental verification and detailed characterization of GK activity of TM1585, the first GK-II family protein with known 3D structure. We used directed mutagenesis and steady-state kinetic analysis to confirm the essential role of the two active site residues Lys-47 and Arg-325 highly conserved in the GK-II family. A novel variant of the three-step serine degradation pathway was inferred in *T. maritima* based on tentative identification of a regulon containing two additional enzymes, serine-pyruvate aminotransferase and hydroxypyruvate reductase (TM1400 and TM1401, respectively). Both enzymatic activities were experimentally verified, and the entire pathway, conversion of serine to 2PG, was validated by its *in vitro* reconstitution.

RESULTS

Comparative genomics of GK-II family and reconstruction of related metabolic pathways

To assess the biological roles of TM1585 and other GK-II enzymes in a context of related metabolic pathways, we performed a comparative genomics survey of completely sequenced bacterial genomes. We used a subsystems-based approach implemented in the SEED genomic platform (http://theseed.uchicago.edu) containing a large collection of integrated genomes and tools for comparative analysis, annotation, and metabolic reconstruction (22). This approach was previously applied for the analysis of various metabolic subsystems and for gene and pathway discovery in a broad range of species (for example, (8, 27, 32)).

The results of this analysis are captured in the SEED subsystem "Glycerate metabolism" available online (http://theseed.uchicago.edu/FIG/subsys.cgi). This subsystem includes all three types of glycerate kinases (GK-I, GK-II, and GK-III) as well as other key enzymes from the described metabolic pathways feeding glycerate to central carbon metabolism, including utilization of serine, glyoxylate, D-glucarate, and tartrate (see Fig. 1B). A condensed version of the subsystem spreadsheet is provided in Supplementary Table S1.

A minimal *serine degradation pathway* (which is also a component of the so-called serine cycle in methylotrophs (3)) includes serine–glyoxylate (or serine–pyruvate) aminotransferase (SAT) and hydroxypyruvate reductase (HPR). The *glyoxylate pathway* is composed of three enzymes, glyoxylate carboligase (GCL), 2-hydroxy-3-oxopropionate reductase (HOPR), and hydroxypyruvate isomerase (HPI). The *tartrate utilization pathway* typically includes a bifunctional tartrate decarboxylase/dehydrogenase enzyme (TDH). The inferred novel pathway of exogenous *D-glycerate utilization* in various γ-proteobacteria (e.g., Altermonadales, Pasteurellales, Pseudomonadales, Vibrionales, and Xanthomonadales) and Firmicutes (Clostridiales and

Lactobacillales) involves a glycerate kinase (GK-I) and a candidate D-glycerate transporter (termed GlyP).

Genome context analysis techniques (implemented in the SEED platform as well as in several other bioinformatics tools) play an important role in subsystems analysis, helping reveal associated pathways, improve the accuracy of gene assignment, and infer functions for some previously uncharacterized genes (for review, see (3)). For example, the observed phylogenetic *occurrence profile* of tentatively assigned glycerate kinase genes revealed an anticorrelation pattern (as defined in (19)), with most species containing genes encoding only one of the three types, GK-I, GK-II, or GK-III (Supplementary Table S1). The GK-I family is the most widely distributed in bacteria, with 159 genes in 135 genomes, predominantly in Gram-positive bacteria (Actinobacteria and the *Bacillus/Clostridium* group) as well as in many β- and γ-proteobacteria (including *E. coli*). It is followed by the GK-II family, 76 genes in 65 genomes, including the *Thermus/Deinococcus* group and most α- and δ-proteobacteria, as well as some β- and γ-proteobacteria. This family dominates in Archaea and Eukaryota. Members of the GK-III family, characteristic of plants, were identified in 30 bacterial genomes, mostly in Cyanobacteria. Such a clear anticorrelation pattern points to the physiological equivalence of all three GK families despite their different reaction specificities (2PG- versus 3PG-forming) that are apparently compensated by the universal presence of PGM interconverting these two metabolites (Fig. 1B).

Identification of gene clustering on the chromosome, another powerful technique of genome context the analysis, provides the most important evidence of their functional coupling (23). The analysis of conserved gene clusters in the genomic neighborhoods of GK-encoding genes revealed multiple cases of their co-localization with genes involved

in the glycerate metabolism (Supplementary Table S1). Remarkably, either one of the nonorthologous GK-I or GK-II genes could be found embedded in otherwise conserved chromosomal gene clusters, for example, in the most abundant *glyoxylate utilization* cluster (encoding orthologous GCL, HPI, and HOPR enzymes).

Several examples of chromosomal clusters observed for GK-II genes in bacteria are illustrated in Fig. 1A. *Tartrate utilization* (TDH) and *serine cycle* (HPR, SAT) genes were found mostly in the chromosomal clusters with GK-II genes. Among a few exceptions are HPR-encoding genes in two *Mycobacterium* species and two γ-proteobacteria (*Methylococcus capsulatus* and *Pseudoalteromonas tunicata*) that occur in clusters with GK-I and GK-III family genes, respectively. In addition to clustering with genes involved in the *upstream* pathways, some of the GK-I and GK-II family genes occurred in clusters with the pyruvate kinase (PYK) gene involved in the *downstream* glycolysis. In the three species of methylotrophic proteobacteria, GK-II genes were found within the extensive methane utilization gene clusters that include serine cycle genes (HPR, SAT) as well as other genes involved in tetrahydrofolate-linked C_1 transfer.

Overall, ~40% of bacterial GK-II genes (30 out of 76) are functionally coupled with genes involved in various pathways of glycerate metabolism via clustering on the chromosome, the most popular being glyoxylate and tartrate utilization clusters. This information allowed us to confidently assert respective pathways in all these species and further project these pathways to other species where GK-II and glycerate metabolism genes occurred in separate chromosomal loci. The observed presence of one or another type of relevant pathway context in nearly all species containing GK-II family genes (clustered or not) provided stronger evidence in support of uniform functional assignment of the entire family.

The phylogenetic tree was constructed for 30 representative bacterial GK-II family proteins with well-defined genome context (Fig. 1C). Color-coding that corresponds to various GK-II related pathways helps emphasize a remarkable diversity of physiologic specialization characteristic of this enzyme family in addition to its taxonomic heterogeneity. Different metabolic pathways are often associated with GK-II enzymes from the same branch, whereas much more divergent members may participate in the same pathway. Some species contain pairs of GK-II paralogs from the distant branches of the tree (and often participating in distinct pathways) pointing to a possible role of horizontal gene transfer, as in the case of two distant GK-II paralogs in *Ralstonia* ssp that are coupled to glyoxylate and tartrate utilization pathways. One of the important observations of this analysis is that sequence similarity or a relative position on the GK-II tree as well as a taxonomic placement of species may not be efficiently used for the accurate projection of physiological functions (or associated pathways) between individual members of the GK-II family. Such a projection requires a more detailed analysis of genomic and functional context, e.g., as in the subsystems-based approach used in this study.

Case study of GK-II related pathway in *T. maritima*

The amino acid sequence of GK-II enzyme TM1585 from *T. maritima* reveals the closest similarity with hyperthermophilic archaeal enzymes, however, in contrast with *P. torridis* (and other thermoacidophilic archaeal species) where the close homolog of TM1585 was characterized (24) as a part of NP-ED pathway, there is no genomic or physiological evidence for the presence of such pathways in *T. maritima.* Therefore, even though an evolutionary history of TM1585 could have included horizontal transfer from

Archaea, in *T. maritima* this gene was adopted for operating in a different functional context. Although no candidate genes of glycerate metabolism could be found in the genomic neighborhood of the TM1585 gene, evidence of its functional coupling with a putative serine degradation operon (TM1400-TM1401) was obtained by the analysis of possible regulatory sites in their upstream DNA regions.

A computational identification of shared regulatory sites and putative regulons is another powerful genome context analysis technique that was successfully applied to reveal functional coupling of genes and operons in many metabolic subsystems and species (26). A conserved palindromic DNA motif (see Fig. 2) was detected in the upstream region of TM1586–TM1585 and TM1400–TM1401 putative operons of *T. maritima* and in the corresponding segments of *T. neapolitana* (the only closely related genome available at the time of this study). Whereas the function of TM1586 is unclear, TM1400 and TM1401, encoding distant homologs of SAT and HPR, respectively, appear to be the only candidate genes in *T. maritima* genome with reliable homology to functional roles captured in the glycerate metabolism subsystem. Further scanning of the upstream regions in *Thermotoga* genomes with a derived DNA profile (termed GK-box, Fig. 2) revealed additional possible members of the same regulon, genes *gldA* (TM0423) and *glpFKP* (TM1429-1430-1431), involved in the glycerol utilization and an operon containing genes *gap* (TM0688) and *pgk-tpiA* (TM0689) involved in glycolysis. While these two pathways do not involve GK-II enzymatic activity, they share a common 2PG intermediate with an inferred serine degradation pathway. It is tempting to speculate that the shared 2PG intermediary metabolite may constitute the actual effector for the entire GK-box regulon. Although a transcription factor for this putative regulon is yet to be established, it does not affect our overall confidence in the main conclusion of this

analysis about the involvement of GK-II enzyme TM1585 in a version of serine degradation pathway together with SAT and HPR enzymes, TM1400 and TM1401.

The proposed pathway illustrated in Fig. 3B, a three-step transformation of serine to 2PG via hydroxypyruvate, is similar to a part of serine cycle previously described in methylotrophic bacteria (3). The only notable difference is due to the apparent absence of glyoxylate in *T. maritima,* as indicated by a draft genome-scale reconstruction of the entire metabolic network of this organism (I. Thiele, personal communication). Glyoxylate is usually considered a main co-substrate in the first step of this pathway, transamination of serine to hydroxypyruvate by SAT. At the same time, some characterized enzymes of this family are known to accept alternative transamination co-substrates such as pyruvate, which (in the absence of glyoxylate) appears to be the most likely component of the *T. maritima* version of serine degradation pathway.

To provide an experimental support for the bioinformatics analysis described above, we performed a detailed enzymatic characterization of TM1585 protein including its reaction specificity, and tested a predicted functional importance of the two conserved residues, Lys47 and Arg325. We also verified the inferred enzymatic activities of TM1400 and TM1401 proteins and performed in vitro reconstitution of the proposed serine degradation pathway as described in the following sections.

Enzymatic activity and active site residues of TM1585, a glycerate 2-kinase from *T. maritima*

We used recombinant TM1585 protein overexpressed in *E. coli* with the N-terminal His_6-tag and purified using Ni-NTA affinity chromatography to test for both types of reaction specificity known for GK enzymes, leading to formation of 2PG and 3PG (see

Fig. 3A). Formation of 2PG product was demonstrated by the coupling assay I using enolase, pyruvate kinase, and lactate dehydrogenase (Fig. 3A). Phosphoglycerate mutase (PGM) catalyzes the reversible 3PG to 2PG transformation, whereas the assay I was irreversible because of the activities of pyruvate kinase and lactate dehydrogenase. The addition of PGM enzyme to the reaction mixture did not affect the overall response, suggesting that the reaction products did not contain any appreciable amounts of 3PG. This conclusion was additionally supported by assay II (Fig. 3A), which showed no indication of 3PG formation in the reaction mixture containing 3-phosphoglycerate kinase and glyceraldehyde-3-phosphate dehydrogenase.

Therefore, TM1585 may be reliably classified as a highly specific 2PG-forming GK enzyme. Based on the data for other diverse members of the GK-II family (3, 24) and a high degree of sequence conservation within the tentative active site area (as discussed below and in (2, 29)), this functional assignment can be safely projected across the entire family (at least 76 members in 65 sequenced bacterial genomes, as well as 12 members in archaeal genomes).

To resolve another potential ambiguity related to contradictory annotations of the GK-II family mentioned above, we tested TM1585 for hydroxypyruvate reductase activity. The spectroscopic assay was performed in both directions, from hydroxypyruvate in the presence of NADH or from glycerate in the presence of NAD^+ (Fig. 3B), giving no indication of their respective activities. A detailed analysis of database records and publications suggests that the propagation of the apparently incorrect hydroxypyruvate reductase annotation over many GK-II homologs originated from the erroneous functional assignment of TtuD involved in tartrate utilization pathway in *Agrobacterium vitis* (4). In a more recent study where this pathway was clarified (Fig.

1B), it was shown that a single enzyme, tartrate dehydrogenase/decarboxylase (TDH), converts tartrate to D-glycerate in three steps with hydroxypyruvate as an intermediate (28). These results suggest that TtuD should have been assigned a GK function, consistent with its homology with other members of the GK-II family.

As is the case with many other *T. maritima* proteins, TM1585 is a thermostable enzyme with maximum enzymatic activity at 80–90°C (Supplementary Figure S3) and shows high activity even during ~5 min incubation at 100°C. However, in contrast to some other enzymes from hyperthermophiles (10, 11), TM1585 has an appreciable activity at 37°C. Therefore, we performed further comparative kinetic studies of wild-type and mutant TM1585 at 37°C, using a continuous coupled assay (Fig. 3B), which is convenient but not amenable to high temperature measurements.

The established steady-state kinetic parameters of TM1585 are shown in Table 1. The values of apparent K_m for D-glycerate (0.15 mM) and ATP (0.095 mM) are comparable to the respective values reported for the GK-II enzyme from *Hyphomicrobium methylovorum* (0.13 mM for both D-glycerate and ATP) (33).

We used site-directed mutagenesis to assess functional importance of the two residues Lys47 and Arg325 highly conserved in the entire GK-II protein family (Supplementary Figure S1) and located in the interdomain region of the TM1585 3D structure. This region is anticipated to comprise the GK-II active site, and, although the catalytic mechanism for this family is yet to be established, conserved positively charged residues are expected to play a key role in the interactions with negatively charged substrates, glycerate, and, especially, ATP (2, 29). Two pairs of TM1585 mutants—K47A, K47R, R325A, and R325K—were obtained and kinetically characterized (Table 1). All these mutations led to a significant decrease in enzymatic activity with most of the

observed effects at the level of apparent k_{cat} values (180-fold for K47R while a milder 17-fold effect for R325A and R325K). The strongest effect was observed in K47A mutant, where individual kinetic parameters could not be reliably measured due to the very low residual activity. Although these data did not allow us to assign a specific role (e.g., in substrate binding) to any of these residues, they confirmed their general importance for catalysis. A 5-fold change of apparent K_m^{ATP} in R325A mutant compared to unchanged K_m^{ATP} of R325K and K47R may, to some extent, reflect the importance of interactions with ATP substrate based on charge or side chain size. Overall, although these data did not provide insight into GK-II mechanism, they support the tentative localization of the active site area in the GK-II family inferred from sequence comparison and TM1585 3D structure.

Experimental validation of the predicted serine degradation pathway in *T. maritima*

Since both TM1400 and TM1401 belong to well-described enzyme families, we did not pursue their detailed characterization and limited our analysis to a qualitative verification of their inferred activities and *in vitro* validation of the entire pathway. This was performed using a panel of coupled assays illustrated in Fig. 3B combined with HPLC-based detection of pathway by-products, ADP and NAD^+ (see Supplementary Figure S4).

The HPR activity of the purified recombinant protein TM1401, an efficient conversion of hydroxypyruvate to D-glycerate, was confirmed by monitoring NADH to NAD^+ conversion at 340 nm. This transformation is nearly irreversible as virtually no enzymatic transformation could be detected in the reverse assay setup, from D-glycerate

to hydroxypyruvate in the presence of NAD^+; this result agrees with reports for other distant members of the HPR family (14).

The PLP-dependent SAT activity of the purified recombinant protein TM1400, a conversion of L-serine to hydroxypyruvate using pyruvate as a co-substrate, was confirmed by coupling this reaction to the consecutive HPR reaction in the presence of excess TM1401 enzyme and NADH (Fig. 3B). The presence of both proteins, TM1400 and TM1401, was necessary and sufficient for quantitative transformation of L-serine to D-glycerate (Table 2). This amounts to *in vitro* reconstitution and validation of the first two steps of the proposed pathway.

Similarly, the last two steps, transformation of hydroxypyruvate to 2PG, were reconstituted in a mixture of two enzymes, TM1401 and TM1585, and monitored by conversion of NADH to NAD^+ and ATP to ADP using HPLC (Table 2 and Supplementary Figure S4). These results, taken together, provide the first confirmation of the physiological role of TM1585, a GK-II family enzyme in *T. maritima,* in serine degradation pathway inferred by comparative genomics and metabolic reconstruction.

DISCUSSION

We combined bioinformatics and experimental techniques to assess enzymatic properties and a possible physiological role of TM1585 protein from *T. maritima*, the first glycerate 2-kinase of the GK-II family with reported 3D structure (29). Members of GK-II family are found in many diverse bacterial species as well as in Archaea and Eukaryota, including mammals (Fig. 1A). GK-II is structurally distinct from the other two described families, GK-I (2), the most abundant family in bacteria, including *E. coli*,

and GK-III, characteristic of plants (1) and cyanobacteria. Some representatives of the GK-II family, including GckA from *M. extorquens* (3), human GLYCK (9), and the enzyme from the archaeon *P. torridus* (24), have been characterized. Nevertheless, many GK-II family members in diverse bacterial genomes still have a misleading hydroxypyruvate reductase (HPR) annotation, a typical example of error propagation in genomic databases originating from the incorrect functional assignment of TtuD protein in *A. vitis* (4).

The detailed enzymatic analysis of the purified recombinant TM1585 presented here allowed us to rule out HPR activity and to confirm its GK activity with physiologically relevant steady-state kinetic parameters. An observed stringent reaction specificity of TM1585 enzyme, exclusive formation of 2PG (and not 3PG) product, together with previous reports for other GK-II family members, supports the unambiguous glycerate 2-kinase assignment for the entire family. Although two other families, GK-I and GK-III, were originally described as 3PG-forming enzymes, the recent data indicate that GK-I family may, in fact, display a glycerate 2-kinase reaction specificity (12). The latter observation is consistent with a possible common evolutionary origin of GK-I and GK-II families that reveal marginal sequence similarities within their respective Rossman-like domains (2).

Unlike many other carbohydrate kinases that belong to large and extensively studied enzyme families, GK-I and GK-II compose distinct structural families with a yet unknown mechanism of action. Crystallographic analysis of TM1585 allowed to take the first steps toward structure–function understanding of the GK-II family by predicting the active site area (2, 29), including two conserved positively charged residues, Lys47 and

Arg325. These residues were tentatively implicated in interactions with negatively charged substrates, ATP and, possibly, glycerate (2, 29).

Our site-directed mutagenesis and steady-state kinetic data (Table 1) confirmed the functional importance of these residues. One of them, Lys47, appears to play a particularly important role in catalysis, as even the K47R mutant conserving the positive charge displays a 180-fold drop in k_{cat}, without any appreciable change in the apparent K_m for either glycerate or ATP. The second and less conserved Arg325 residue (replaced by proline in ~25% of all compared bacterial enzymes) may be involved in charge or side chain interactions with ATP (but not glycerate) as suggested by a 5-fold increase of the apparent K_m^{ATP} observed in R325A but not in R325K mutant. Although an accurate mechanistic interpretation of these data awaits further analysis, an observed functional conservation of these residues provides an additional support for the presumed conservation of the biochemical function within the entire GK-II family.

A remarkable homogeneity of substrate specificity across the GK-II family is in contrast with other large families of carbohydrate kinases, e.g., the FGGY protein family (Pfam accession number PF00294), which contains representatives with widely different substrate preferences toward a broad range of distinct sugars, including xylulose kinase TM0116 (EC 2.7.1.17), ribulokinase TM0284 (EC 2.7.1.16), glycerol kinase TM1430 (EC 2.7.1.30), gluconokinase TM0443 (EC 2.7.1.12), and rhamnulokinase TM1073 (EC 2.7.1.5) in *T. maritima* (unpublished results). In addition to the experimental evidence accumulated for several divergent members of the GK-II family, its functional homogeneity is strongly supported by the metabolic reconstruction and genome context analysis performed in this study. A significant fraction (~40%) of GK-II family genes in a collection of diverse bacterial genomes are clustered on the chromosome with genes

involved in glycerate metabolism (Fig. 1), providing strong support for their functional assignment and for the assertion of respective metabolic pathways.

The comparative analysis of bacterial genomes included in the "glycerate metabolism" subsystem (Supplementary Table S1) revealed a remarkable diversity of pathways that involve GK-II enzymes (Fig. 1). Among them, most frequent are the pathways of glyoxylate, serine, and tartrate utilization, whereas utilization of D-glucarate and D-glycerate are relatively rare for GK-II while being quite common for GK-I family enzymes. An observed mosaic phylogenetic distribution of genes corresponding to all three enzyme families—GK-I, GK-II, and GK-III—that are often involved in the same pathways and even in similarly organized chromosomal clusters confirms the equivalence of their functional roles *in vivo*.

An inventory analysis of genes associated with all functional roles included in the subsystem allowed us to expand pathway assertions toward many other genomes where GK-II genes are not involved in any suggestive chromosomal clusters. In the case of *T. maritima*, a remote operon encoding homologs of SAT and HPR enzymes (TM1400–TM1401) was deemed the only possible functional context for GK-II enzyme (TM1585). The inferred three-step serine degradation pathway was further supported by the identification of conserved putative regulatory sites in the upstream region of the respective genomic loci in *T. maritima* and *T. neapolitana* (Fig. 2).

Importantly, this analysis allowed us to suggest specific functional assignments for TM1400 and TM1401 genes that belong to large enzyme families (PLP-dependent aminotransferase and D-isomer specific 2-hydroxyacid dehydrogenase, respectively) with wide variations in substrate specificity between individual characterized representatives. Due to a divergent phylogenetic placement of *T. maritima* proteins, their precise substrate

specificity could not be reliably predicted based solely on sequence similarity. Indeed, the current annotations of these proteins in most public archives are either imprecise (e.g., putative aminotransferase for TM1400) or incorrect (D-3-phosphoglycerate dehydrogenase).

Both inferred activities, SAT and HPR, were confirmed for the purified recombinant proteins TM1400 and TM1401, respectively, using specific assays (Fig. 3B). Although glyoxylate is considered a major physiological co-substrate for other SAT enzymes previously described as serine-glyoxylate aminotransferases (EC 2.6.1.45), it does not appear to be a relevant intermediate in *T. maritima* metabolic network. At the same time, pyruvate, an important intermediary metabolite in *T. maritima,* was proven to be an efficient transamination co-substrate of TM1400, which should be formally classified as serine-pyruvate aminotransferase (EC 2.6.1.51). A challenge of distinguishing between biochemical and physiologically relevant activities is rather common for enzyme families with broad substrate specificities. Likewise, HPR enzymes (EC 1.1.1.81) from several species were shown to display an appreciable glyoxylate reductase (EC 1.1.1.26) activity. Although both of these activities are displayed *in vitro* by TM1401, only one of them, HPR, appears to be physiologically relevant for *T. maritima*.

Finally, the results obtained for two overlapping pairs of coupled reactions (TM1400 + TM1401 and TM1401 + TM1585) provided us with an experimental validation of the inferred three-step serine degradation pathway (Table 2). Despite the obvious shortcomings of *in vitro* data, in combination with bioinformatic analysis they constitute sufficient evidence for confident inclusion of this pathway in the reconstruction of the *T. maritima* metabolic network. Taking into account an organotrophic life-style of

T. maritima (13), a possible physiological role of this pathway may be in utilization of exogenous serine from its environment enriched with amino acids and other carbon and energy sources.

In summary, the key results of this study obtained by applying a subsystems-based approach (22) to the analysis of bacterial metabolic pathways that involve members of GK-I, GK-II, and GK-III enzyme families are as follows: (i) >1,000 individual genes from ~200 complete or nearly complete bacterial genomes and representing 12 distinct functional roles (mostly enzymes) were reliably and consistently annotated; (ii) a functional context of 76 members of GK-II family identified in 65 diverse bacterial species was analyzed in detail, and specific pathways (or groups of pathways) were asserted in most of these species; (iii) in the *T. maritima* case study, a novel putative regulon was identified covering an inferred serine degradation pathway and two other pathways, utilization of glycerol and a part of glycolysis that share a common intermediary metabolite (and a likely effector) 2PG; (iv) a proposed version of the serine degradation pathway in *T. maritima* implemented by the three enzymes—pyruvate-utilizing SAT (TM1400), HPR (TM1401), and GK-II (TM1585)—was validated by *in vitro* reconstitution. A detailed experimental characterization of the glycerate 2-kinase TM1585, the main focus of this study, confirmed its substrate and reaction specificity and the functional importance of the two putative active site residues, K47 and R237, largely conserved within the GK-II family.

MATERIALS AND METHODS

Genome resources and bioinformatics tools. Metabolic reconstruction, genome context analysis (chromosomal clustering and phylogenetic profiling), and subsystem encoding including annotations of relevant genes in a collection of ~400 complete and almost complete genomes was performed using the SEED genomic platform (http://theseed.uchicago.edu/FIG/index.cgi) as previously described (25, 29). The subsystems-based approach to genome analysis and the extensive use of genome context allows to significantly improve the accuracy of gene functional assignment and pathway reconstruction (20). The results of this analysis are captured in the novel subsystem, "*Glycerate metabolism*," available on-line (http://theseed.uchicago.edu/FIG/subsys.cgi?user=&ssa_name=Glycerate_metabolism&request=show_ssa). Genomes were uploaded from GenBank (http://www.ncbi.nlm.nih.gov/Genbank/). Preliminary genome sequence data for *Thermotoga neapolitana* was obtained from The Institute for Genomic Research (http://www.tigr.org). Tertiary structures were from PDB (http://www.rcsb.org/). ClustalX (30) and PHYLIP (7) were used to construct multiple protein alignments and phylogenetic trees by the maximum likelihood method (16). GK-box regulatory DNA motif was identified by an iterative signal detection procedure implemented in the SignalX program (24); additional GK-box regulatory sites were located in the *Thermotoga* genomes using the Genome Explorer software (17).

Bacterial strains, plasmids, and reagents. *E. coli* strain DH5α (Invitrogen, Carlsbad, CA) was used for gene cloning, and BL21 and BL21/DE3 (Gibco-BRL, Rockville, MD) were used for protein overexpression. A pET-derived vector containing the T7 promoter, His_6 tag, and tobacco etch virus-protease cleavage site (20), was used

for protein expression. The resulting plasmid was transformed into *E. coli* BL21/DE3. Enzymes for PCR and DNA manipulations were from New England Biolabs Inc. (Beverly, MA). Plasmid purification kits were from Promega (Madison, WI). PCR purification kits and nickel-nitrilotriacetic acid (Ni-NTA) resin were from QIAGEN Inc. (Valencia, CA). Oligonucleotides for PCR and sequencing were synthesized by Sigma-Genosys (Woodlands, TX). All other chemicals, including the assay components D-glycerate, 3-hydroxypyruvate, L-serine, pyruvate, glyoxylate, NADH, NADPH, NAD^+, $NADP^+$, ATP, phosphoenolpyruvate, enolase, lactate dehydrogenase, pyruvate kinase, 3-phosphoglycerate kinase, and glyceraldehyde-3-phosphate dehydrogenase were purchased from Sigma-Aldrich (St. Louis, MO). The plasmids harboring TM1585 (GK-II) or TM1400 (SAT) gene with arabinose promoter and His_6-tag (29) were a kind gift from Dr. S. Lesley at the Joint Center for Structural Genomics (JCSG), and were then transformed into *E. coli* BL21.

PCR amplification and cloning. TM1401 (HPR) gene from *Thermotoga maritima* MSB8 was amplified using the following primers:

5′-ggcg**ccATGG**CGAGATACAGAGTGCACGTGAACGATCCTCTCGATAAAGAG

and 3′-gag**gtcgac**TCAAATTCCCAGTTCTTTGAAAATCTTCTCCACGAGTTCTAT.

Introduced restriction sites (*Nco*I and *Pci*I for the 5′-end and *Sal*I for the 3′-end) are shown in boldface; mutations and added nucleotides are shown in lowercase. PCR amplification was performed using *T. maritima* MSB8 genomic DNA. PCR fragments were cloned into the pET-derived expression vector cleaved by *Nco*I and *Sal*I. Selected clones were confirmed by DNA sequence analysis.

For site-directed mutagenesis of TM1585, the following PCR primers were used:

5′-cggagg**acATGT**TTGATCCTGAATCCTTGAAG and

3′-gacgc**gtcgac**CTAGACGATGAGGCCTATTATCAAG for the full-sized coding region;

5′-CTCGTTGCCGTTGGGgcAGCAGCGTGGCGAATGGC and

3′-GCCATTCGCCACGCTGCTgcCCCAACGGCAACGAG for the K47A mutant;

5′-CTCGTTGCCGTTGGGAgAGCAGCGTGGCGAATGGC and

3′-GCCATTCGCCACGCTGCTcTCCCAACGGCAACGAG for the K47R mutant;

5′-GGAAACGGCATCGGAGGAgcAAACCAAGAACTTGC and

3′-GCAAGTTCTTGGTTTgcTCCTCCGATGCCGTTTCC for the R325A mutant;

5′-GGAAACGGCATCGGAGGAAagAACCAAGAACTTGC and

3′-GCAAGTTCTTGGTTctTTCCTCCGATGCCGTTTCC for the R325K mutant.

Site-directed mutagenesis. Amino acid substitutions (K47A, K47R, R325A, and R325K) of TM1585 were generated using the sequential PCR steps technique. Briefly, mutant primers (sense and antisense) containing the separate base substitutions were synthesized. In the first step, two separate PCR runs were performed with two sets of primers, 5′-end-flanking and antisense mutant primers as well as 3′-end-flanking and sense mutant primers, and 10 ng of the expression plasmid encoding full-sized TM1585. Both amplified mutated fragments were purified, mixed in a 1:1 molar ratio, and used as the template for a second step of amplification with flanking primers under standard conditions to produce the full-length mutated fragment.

Protein overexpression and purification. Recombinant proteins were overexpressed as N-terminal fusions with a His_6 tag in *E. coli* strain BL21 or BL21/DE3. For expression of TM1585 and TM1400, cells were grown on TB media (24 g/L yeast extract and 12 g/L tryptone) containing 1% glycerol and 50 mM Mops, pH 7.6, induced by 0.15% arabinose, and harvested after 3 h shaking at 37°C. For expression of TM1401

and TM1585 mutants, cells were grown on LB media to OD_{600} = 0.8 at 37°C, induced by 0.2mM IPTG, and harvested after 12 h shaking at 20°C. Protein purification was performed using rapid Ni-NTA agarose minicolumn protocol as described (21). Briefly, harvested cells were resuspended in 20 mM HEPES buffer pH 7 containing 100 mM NaCl, 0.03% Brij 35, and 2 mM β-mercaptoethanol supplemented with 2 mM phenylmethylsulfonyl fluoride and a protease inhibitor cocktail (Sigma-Aldrich). Lysozyme was added to 1 mg/mL, and the cells were lyzed by freezing-thawing followed by sonication. After centrifugation at 18,000 rpm, the Tris-HCl buffer (pH 8) was added to the supernatant (50 mM, final concentration), and it was loaded onto a Ni-nitrilotriacetic acid agarose column (0.2 ml). After washing with the starting buffer containing 1 M NaCl and 0.3% Brij-35, bound proteins were eluted with 0.3 ml of the starting buffer containing 250 mM imidazole. For purification of TM1400, 0.1 mM pyridoxal 5′-phosphate was added to the buffers and the protein mixture was heated for 10 min at 65°C to weaken partial contamination by *E. coli* proteins because of the intrinsic thermostability of *T. maritima* proteins. Protein size, expression level, distribution between soluble and insoluble forms, and extent of purification were monitored by SDS-PAGE. The soluble proteins for TM1401 and TM1585 were obtained with high yield (>1mg from 50-ml culture) and purified to >90% by SDS-PAGE (see Supplementary Fig. S2)

Enzyme assays. In all coupled assays, the change in NADH or NADPH absorbance was monitored at 340 nm using a Beckman DTX-880 multimode microplate reader. An NADH or NADPH extinction coefficient of 6.22 $mM^{-1}cm^{-1}$ was used for rate calculation. Initial rate calculations were performed with Multimode Detection Software (Beckman). Kinetic data for wild-type and mutant TM1585 were analyzed using the XLfit4 program

(IDBS). A standard Michaelis–Menten model was used to determine the apparent values of k_{cat} and K_m . Details of individual assays are provided below.

Glycerate kinase activity was assayed by coupling the formation of ADP to the oxidation of NADH to NAD^+ via pyruvate kinase and lactate dehydrogenase and monitored at 340 nm. Briefly, 0.2–0.4 µg of purified glycerate kinase was added to 200 µL of reaction mixture containing 50 mM Tris buffer (pH 7.5), 10 mM $MgSO_4$, 1.2 mM ATP, 1.2 mM phosphoenolpyruvate, 0.3 mM NADH, 1.2 U of pyruvate kinase, 1.2 U of lactate dehydrogenase, and 1 mM D-glycerate at 37°C. No activity was detected in a control experiment, in which an unrelated gene (TM1602) was expressed in the same vector and purified in parallel. For determination of the apparent k_{cat} and the K_m of TM1585 and the mutants, D-glycerate or ATP concentration was varied in the range of 0.05 to 5 mM in the presence of saturating concentration of the other substrate (ATP or D-glycerate, 2mM). Temperature dependence of enzyme activity was measured between 37°C and 95°C using a discontinuous assay. The assay mixture (200 µL) contained 50 mM Tris-HCl, pH 7.5 (adjusted at the respective temperatures), 2 mM D-glycerate, 2 mM ATP, and 20 mM $MgCl_2$, which ensured specific activities close to V_{max}. After pre-incubation, the reaction was started by adding glycerate kinase, incubated for 5 min, and stopped by rapid addition of 20 µl of ice-cold 50% (v/v) perchloric acid. After rapid vortexing, the mixture was kept on ice for 10 min and neutralized with 30% KOH, and the resulting precipitate was then removed by centrifugation. To 100 µl of the supernatant, 400 µl of 50 mM Tris-HCl, pH 7.5, containing 2 mM PEP and 0.25 mM NADH was added. The amount of ADP formed by the glycerate kinase reaction was quantified by adding a mixture of pyruvate kinase and lactate dehydrogenase and following the oxidation of NADH at 340 nm.

Phosphorylation specificity of glycerate kinase was performed using two assays (33). (I) Formation of 2PG was detected by coupling to the oxidation of NADH to NAD^+ via consecutive enolase, pyruvate kinase, and lactate dehydrogenase reactions and monitoring at 340 nm (Fig. 3A). The reaction mixture (200 µL) contained 50 mM Tris (pH 7.5), 20 mM $MgCl_2$, 1 mM D-glycerate, 2 mM ATP, 0.3 mM NADH, 4.5 U of enolase, 7.2 U of pyruvate kinase, 8.1 U of lactate dehydrogenase, and 6 µg of purified glycerate kinase. To test for the presence of the alternative 3PG product, phosphoglycerate mutase (10.0 U) was added to the same reaction mixture in a parallel sample. (II) Formation of 3-phosphoglycerate was tested by adding 3-phosphoglycerate kinase and glyceraldehyde-3-phosphate dehydrogenase and monitoring the oxidation of NADH to NAD^+ at 340 nm (Fig. 3A). The reaction mixture (200 µL) contained 50 mM sodium phosphate buffer (pH 8.0), 20 mM $MgCl_2$, 1 mM D-glycerate, 2 mM ATP, 0.3 mM NADH, 8.1 U of glyceraldehyde-3-phosphate dehydrogenase, 9.0 U of 3-phosphoglycerate kinase, and 6 µg of purified glycerate kinase.

Hydroxypyruvate reductase activity was assayed by monitoring the decrease in absorbance at 340 nm due to the conversion of NADH to NAD^+. Briefly, 5–10 µg of purified hydroxypyruvate reductase was added to 200 µl of reaction mixture containing 50 mM sodium phosphate buffer (pH 7.5), 0.3 mM NADH or NADPH, and 2 mM 3-hydroxypyruvate at 37°C. No activity was detected in a control experiment, in which an unrelated gene (TM1602) was expressed in the same vector and purified in parallel. The reverse reaction of hydroxypyruvate reductase (i.e., glycerate dehydrogenase) was determined by measuring the reduction of NAD^+ to NADH. The reaction mixture (200 µL) contained 50 mM Tris buffer (pH 8.0), 1 mM D-glycerate, 0.3 mM NAD^+, and 10 µg of purified glycerate dehydrogenase.

PLP-dependent serine-pyruvate aminotransferase activity was assayed by coupling to hydroxypyruvate reductase reaction and monitoring the oxidation of NADH to NAD^+ at 340 nm. The reaction mixture (200 µL) contained 50 mM sodium phosphate buffer (pH 7.5), 0.1 mM pyridoxal 5′-phosphate, 0.3 mM NADH, 2 mM pyruvate, 2 mM L-serine, and 10–20 µg of purified serine-pyruvate aminotransferase and hydroxypyruvate reductase. For testing glyoxylate as an alternative substrate, pyruvate was exchanged for 2 mM glyoxylate. No activity was detected in a control experiment, in which an unrelated gene (TM1602) was expressed in the same vector and purified in parallel.

In vitro *reconstitution of serine degradation pathway.* Conversion of L-serine to D-glycerate by a mixture of purified serine-pyruvate aminotransferase (TM1400) and hydroxypyruvate reductase (TM1401) was determined by monitoring the decrease in absorbance at 340 nm due to the conversion of NADH to NAD^+, which was described above as serine-pyruvate aminotransferase activity assay. In control samples one enzyme was excluded from the mixture.

Conversion of hydroxypyruvate to 2-phosphoglycerate by a mixture of purified hydroxypyruvate reductase (TM1401) and glycerate kinase (TM1585) was determined by monitoring the conversion of NADH to NAD^+ and ATP to ADP using HPLC. The reaction mixture contained 50 mM sodium phosphate buffer (pH 7.5), 20 mM $MgCl_2$, 1 mM 3-hydroxypyruvate, 1 mM NADH, 1 mM ATP, and 5–20 µg of purified hydroxypyruvate reductase and glycerate kinase. In control samples one enzyme was excluded from the mixture. After 2 hour of incubation at 37°C, proteins were removed by microultrafiltration using Microcon YM-10 centrifugal filters (Amicon, Bedford, MA), and the filtrates were analyzed using a Shimadzu HPLC system with LC-10AD solvent

delivery system, SIL-20A auto sampler, and SPD-20AD UV/Vis detector. The separation of nucleotides was performed on a Supelco LC-18-T (15 cm × 4.6 mm, 3 μm particle size) chromatographic column equipped with Supelguard LC-18-T (2.0 cm × 4.0 mm, 5 μm particle size) guard column (Supelco, Bellefonte, PA) at room temperature with detection at 254 nm. Elution was performed at 1 mL/min by 1.5–30% gradient of methanol in 100 mM potassium phosphate, pH 6.0, with 8 mM tetrabutylammonium bromide.

ACKNOWLEDGMENTS

We are grateful to Dr. S. Lesley at the Joint Center of Structural Genomics for providing expression clones of *T. maritima* proteins and to Dr. S. Krishna for the help in the analysis of TM1585 3D structure. We want to thank Dr. R. Overbeek and his colleagues at Fellowship for Interpretation of Genomes (FIG, Illinois) for their help with the use of The SEED genomic resource, Drs. M. Gelfand and A. Mironov (IITP, Moscow) for their help with the analysis of regulons, and Dr. L. Sorci (BIMR, San Diego) for his help with the HPLC assay. This work was partially supported by the DOE grant DE-FG02-07ER64384, "Integrated Genome-Based Studies of Shewanella Ecophysiology."

REFERENCES

1. **Boldt, R., C. Edner, U. Kolukisaoglu, M. Hagemann, W. Weckwerth, S. Wienkoop, K. Morgenthal, and H. Bauwe.** 2005. D-GLYCERATE 3-KINASE, the last unknown enzyme in the photorespiratory cycle in Arabidopsis, belongs to a novel kinase family. Plant Cell **17:**2413-20.
2. **Cheek, S., K. Ginalski, H. Zhang, and N. V. Grishin.** 2005. A comprehensive update of the sequence and structure classification of kinases. BMC Struct Biol **5:**6.
3. **Chistoserdova, L., and M. E. Lidstrom.** 1997. Identification and mutation of a gene required for glycerate kinase activity from a facultative methylotroph, Methylobacterium extorquens AM1. J Bacteriol **179:**4946-8.
4. **Crouzet, P., and L. Otten.** 1995. Sequence and mutational analysis of a tartrate utilization operon from Agrobacterium vitis. J Bacteriol **177:**6518-26.
5. **Cusa, E., N. Obradors, L. Baldoma, J. Badia, and J. Aguilar.** 1999. Genetic analysis of a chromosomal region containing genes required for assimilation of allantoin nitrogen and linked glyoxylate metabolism in Escherichia coli. J Bacteriol **181:**7479-84.
6. **Doughty, C. C., J. A. Hayashi, and H. L. Guenther.** 1966. Purification and properties of D-glycerate 3-kinase from Escherichia coli. J Biol Chem **241:**568-72.
7. **Felsenstein, J.** 1981. Evolutionary trees from DNA sequences: a maximum likelihood approach. J Mol Evol **17:**368-76.
8. **Gerdes, S. Y., O. V. Kurnasov, K. Shatalin, B. Polanuyer, R. Sloutsky, V. Vonstein, R. Overbeek, and A. L. Osterman.** 2006. Comparative genomics of NAD biosynthesis in cyanobacteria. J Bacteriol **188:**3012-23.
9. **Guo, J. H., S. Hexige, L. Chen, G. J. Zhou, X. Wang, J. M. Jiang, Y. H. Kong, G. Q. Ji, C. Q. Wu, S. Y. Zhao, and L. Yu.** 2006. Isolation and characterization of the human D-glyceric acidemia related glycerate kinase gene GLYCTK1 and its alternatively splicing variant GLYCTK2. DNA Seq **17:**1-7.
10. **Hansen, T., M. Musfeldt, and P. Schonheit.** 2002. ATP-dependent 6-phosphofructokinase from the hyperthermophilic bacterium Thermotoga maritima: characterization of an extremely thermophilic, allosterically regulated enzyme. Arch Microbiol **177:**401-9.
11. **Hansen, T., and P. Schonheit.** 2003. ATP-dependent glucokinase from the hyperthermophilic bacterium Thermotoga maritima represents an extremely thermophilic ROK glucokinase with high substrate specificity. FEMS Microbiol Lett **226:**405-11.
12. **Hubbard, B. K., M. Koch, D. R. Palmer, P. C. Babbitt, and J. A. Gerlt.** 1998. Evolution of enzymatic activities in the enolase superfamily: characterization of the (D)-glucarate/galactarate catabolic pathway in Escherichia coli. Biochemistry **37:**14369-75.
13. **Huser, B., Patel, BKC, Daniel, RM, and Morgan, HW.** 1986. Isolation and characterization of a novel extremely thermophilic anaerobic chemo-organotrophic eubacterium. FEMS Microbiol. Lett. **37:**121-127.
14. **Izumi, Y., T. Yoshida, H. Kanzaki, S. Toki, S. S. Miyazaki, and H. Yamada.** 1990. Purification and characterization of hydroxypyruvate reductase from a serine-producing methylotroph, Hyphomicrobium methylovorum GM2. Eur J Biochem **190:**279-84.
15. **Katayama, H., Y. Kitagawa, and E. Sugimoto.** 1980. Purification of rat liver glycerate kinase and studies of its enzymatic and immunological properties. J Biochem (Tokyo) **88:**765-73.
16. **Matsuda, H.** 1996. Protein phylogenetic inference using maximum likelihood with a genetic algorithm. Pac Symp Biocomput**:**512-23.
17. **Mironov, A. A., N. P. Vinokurova, and M. S. Gel'fand.** 2000. [Software for analyzing bacterial genomes]. Mol Biol (Mosk) **34:**253-62.
18. **Monterrubio, R., L. Baldoma, N. Obradors, J. Aguilar, and J. Badia.** 2000. A common regulator for the operons encoding the enzymes involved in D-galactarate, D-glucarate, and D-glycerate utilization in Escherichia coli. J Bacteriol **182:**2672-4.
19. **Morett, E., J. O. Korbel, E. Rajan, G. Saab-Rincon, L. Olvera, M. Olvera, S. Schmidt, B. Snel, and P. Bork.** 2003. Systematic discovery of analogous enzymes in thiamin biosynthesis. Nat Biotechnol **21:**790-5.
20. **Osterman, A., N. V. Grishin, L. N. Kinch, and M. A. Phillips.** 1994. Formation of functional cross-species heterodimers of ornithine decarboxylase. Biochemistry **33:**13662-7.

21. **Osterman, A. L., D. V. Lueder, M. Quick, D. Myers, B. J. Canagarajah, and M. A. Phillips.** 1995. Domain organization and a protease-sensitive loop in eukaryotic ornithine decarboxylase. Biochemistry **34:**13431-6.
22. **Overbeek, R., T. Begley, R. M. Butler, J. V. Choudhuri, H. Y. Chuang, M. Cohoon, V. de Crecy-Lagard, N. Diaz, T. Disz, R. Edwards, M. Fonstein, E. D. Frank, S. Gerdes, E. M. Glass, A. Goesmann, A. Hanson, D. Iwata-Reuyl, R. Jensen, N. Jamshidi, L. Krause, M. Kubal, N. Larsen, B. Linke, A. C. McHardy, F. Meyer, H. Neuweger, G. Olsen, R. Olson, A. Osterman, V. Portnoy, G. D. Pusch, D. A. Rodionov, C. Ruckert, J. Steiner, R. Stevens, I. Thiele, O. Vassieva, Y. Ye, O. Zagnitko, and V. Vonstein.** 2005. The subsystems approach to genome annotation and its use in the project to annotate 1000 genomes. Nucleic Acids Res **33:**5691-702.
23. **Overbeek, R., N. Larsen, G. D. Pusch, M. D'Souza, E. Selkov, Jr., N. Kyrpides, M. Fonstein, N. Maltsev, and E. Selkov.** 2000. WIT: integrated system for high-throughput genome sequence analysis and metabolic reconstruction. Nucleic Acids Res **28:**123-5.
24. **Reher, M., M. Bott, and P. Schonheit.** 2006. Characterization of glycerate kinase (2-phosphoglycerate forming), a key enzyme of the nonphosphorylative Entner-Doudoroff pathway, from the thermoacidophilic euryarchaeon Picrophilus torridus. FEMS Microbiol Lett **259:**113-9.
25. **Reher, M., and P. Schonheit.** 2006. Glyceraldehyde dehydrogenases from the thermoacidophilic euryarchaeota Picrophilus torridus and Thermoplasma acidophilum, key enzymes of the non-phosphorylative Entner-Doudoroff pathway, constitute a novel enzyme family within the aldehyde dehydrogenase superfamily. FEBS Lett **580:**1198-204.
26. **Rodionov, D. A.** 2007. Comparative Genomic Reconstruction of Transcriptional Regulatory Networks in Bacteria. Chem Rev.
27. **Rodionov, D. A., O. V. Kurnasov, B. Stec, Y. Wang, M. F. Roberts, and A. L. Osterman.** 2007. Genomic identification and in vitro reconstitution of a complete biosynthetic pathway for the osmolyte di-myo-inositol-phosphate. Proc Natl Acad Sci U S A **104:**4279-84.
28. **Ruszczycky, M. W., and V. E. Anderson.** 2004. Tartrate dehydrogenase reductive decarboxylation: stereochemical generation of diastereotopically deuterated hydroxymethylenes. Bioorg Chem **32:**51-61.
29. **Schwarzenbacher, R., D. McMullan, S. S. Krishna, Q. Xu, M. D. Miller, J. M. Canaves, M. A. Elsliger, R. Floyd, S. K. Grzechnik, L. Jaroszewski, H. E. Klock, E. Koesema, J. S. Kovarik, A. Kreusch, P. Kuhn, T. M. McPhillips, A. T. Morse, K. Quijano, G. Spraggon, R. C. Stevens, H. van den Bedem, G. Wolf, K. O. Hodgson, J. Wooley, A. M. Deacon, A. Godzik, S. A. Lesley, and I. A. Wilson.** 2006. Crystal structure of a glycerate kinase (TM1585) from Thermotoga maritima at 2.70 A resolution reveals a new fold. Proteins **65:**243-8.
30. **Thompson, J. D., T. J. Gibson, F. Plewniak, F. Jeanmougin, and D. G. Higgins.** 1997. The CLUSTAL_X windows interface: flexible strategies for multiple sequence alignment aided by quality analysis tools. Nucleic Acids Res **25:**4876-82.
31. **Van Schaftingen, E.** 1989. D-glycerate kinase deficiency as a cause of D-glyceric aciduria. FEBS Lett **243:**127-31.
32. **Yang, C., D. A. Rodionov, X. Li, O. N. Laikova, M. S. Gelfand, O. P. Zagnitko, M. F. Romine, A. Y. Obraztsova, K. H. Nealson, and A. L. Osterman.** 2006. Comparative genomics and experimental characterization of N-acetylglucosamine utilization pathway of Shewanella oneidensis. J Biol Chem **281:**29872-85.
33. **Yoshida, T., K. Fukuta, T. Mitsunaga, H. Yamada, and Y. Izumi.** 1992. Purification and characterization of glycerate kinase from a serine-producing methylotroph, Hyphomicrobium methylovorum GM2. Eur J Biochem **210:**849-54.

TABLE 1. Kinetic parameters of wild-type TM1585 and its derivatives obtained by site-drected mutagenesis

Proteins	k_{cat} (s^{-1})[a]	$K_{m,ATP}$ (mM)[b]	k_{cat} / $K_{m,ATP}$ ($M^{-1}s^{-1}$)	$K_{m,glycerate}$ (mM)[b]
TM1585	14.4 ± 0.4	0.095 ± 0.009	$1.5 \times 10^5 \pm 0.1 \times 10^5$	0.15 ± 0.03
R325K	0.84 ± 0.02	0.11 ± 0.01	$7.7 \times 10^3 \pm 0.7 \times 10^3$	0.13 ± 0.02
R325A	0.90 ± 0.03	0.47 ± 0.05	$1.9 \times 10^3 \pm 0.2 \times 10^3$	0.19 ± 0.05
K47R	0.08 ± 0.01	0.13 ± 0.02	$6.7 \times 10^2 \pm 1.3 \times 10^2$	0.20 ± 0.04
K47A	nd	nd	0.15 ± 0.04	nd

[a] k_{cat} values for ATP are presented, and similar values were found for glycerate. nd, not determined. All measurements were performed at 37°C.
[b] $K_{m(app)}$ was obtained by varying the substrate concentration at saturating concentration of the second substrate (2mM for both ATP and D-glycerate).

TABLE 2. *In vitro* reconstitution of serine degradation pathway using recombinant purified *T. maritima* enzymes.

Substrates added	Enzymes added	Conversion of NADH to NAD^+ and/or ATP to ADP
L-Serine and pyruvate[a]	SAT and HPR	+
	SAT	–
	HPR	–
3-hydroxypyruvate[b]	HPR and GK-II	+
	HPR	–
	GK-II	–

[a]Conversion of L-serine to D-glycerate by a mixture of SAT (TM1400) and HPR (TM1401) enzymes was determined by monitoring the decrease in absorbance at 340 nm due to the conversion of NADH to NAD^+ (see the assay shown in Fig. 3B).
[b]Conversion of hydroxypyruvate to 2-phospho-D-glycerate by a mixture of HPR (TM1400) and GK-II (TM1585) was detected by monitoring the conversion of NADH to NAD^+ and ATP to ADP using HPLC.

Figure Legends

FIG. 1. Genomic and functional context of glycerate kinase enzymes in bacteria. In all panels matching colors are used to mark components of distinct pathways related to glycerate metabolism.

(A) Examples of chromosomal clusters containing GK-II genes in bacteria. Genes (shown by arrows) from the same metabolic pathway are marked by matching colors. Transcriptional regulators are shown in black. The species with experimentally characterized pathways and enzymes are underlined. The presence of common regulatory site upstream of the serine degradation genes in *T. maritima* is shown by black dots.

(B) Reconstruction of metabolic pathways involving D-glycerate. Abbreviations for pathway intermediates (in circles and ovals) are given at the top. Abbreviations for enzymes: GK, glycerate kinase; SAT, serine aminotransferase; HPR, hydroxypyruvate reductase; GlyP, glycerate transporter; GADH, glyceraldehyde dehydrogenase; HPI, hydroxypyruvate isomerase; GCL, glyoxylate carboligase; HOPR, 2-hydroxy-3-oxopropionate reductase; GARL, 2-dehydro-3-deoxyglucarate aldolase; TDH, tartrate dehydrogenase/decarboxylase; PGK, 3-phosphoglycerate kinase; PGM, phosphoglycerate mutase; ENO, enolase; PYK, pyruvate kinase. Different metabolic pathways and respective enzymes are denoted by background color arrows and boxes marked by the same matching colors.

(C) Phylogenetic tree of selected GK-II family proteins in bacteria whose biological role was tentatively identified using genome context analysis. Background colors reflect chromosomal clustering of GK-II genes with the genes from the respective

metabolic pathways. Clustering of GK-II with *pyk* genes is marked by red lines. Branching point of GK-II proteins from Eukaryotes and Archaea are indicated and colored according to their biological roles reported elsewhere. Abbreviations for taxonomic groups: α, β, γ, and δ denote α-, β-, γ-, and δ-proteobacteria; Act., Actinobacteria; T/D, *Thermus/Deinococcus* group.

FIG. 2. Candidate regulatory sites (GK-box) of GK-II and other members of a putative regulon in *Thermotoga* species. Left, GK-boxes are shown by black circles, and genes are shown by arrows. Right, sequence logo for GK-box consensus and individual GK-boxes.

FIG. 3. Enzymatic reactions and assays. (A) Coupled assays were used to establish the reaction specificity of D-glycerate phosphorylation by TM1585: (i) detection of 2PG was monitored at 340 nm by coupling to NADH oxidation via three consecutive reactions catalyzed by ENO, PYK, and lactate dehydrogenase (LDH); (ii) no indication of 3PG formation was obtained in the alternative assay with addition of PGK and glyceraldehyde-3-phosphate dehydrogenase (GAPDH). (B) Biochemical transformations in the *T. maritima* serine degradation pathway and the assays used to assess enzymatic activities of GK-II (TM1585) and of the two additional enzymes, SAT (TM1400) and HPR (TM1401).

Figure 1.

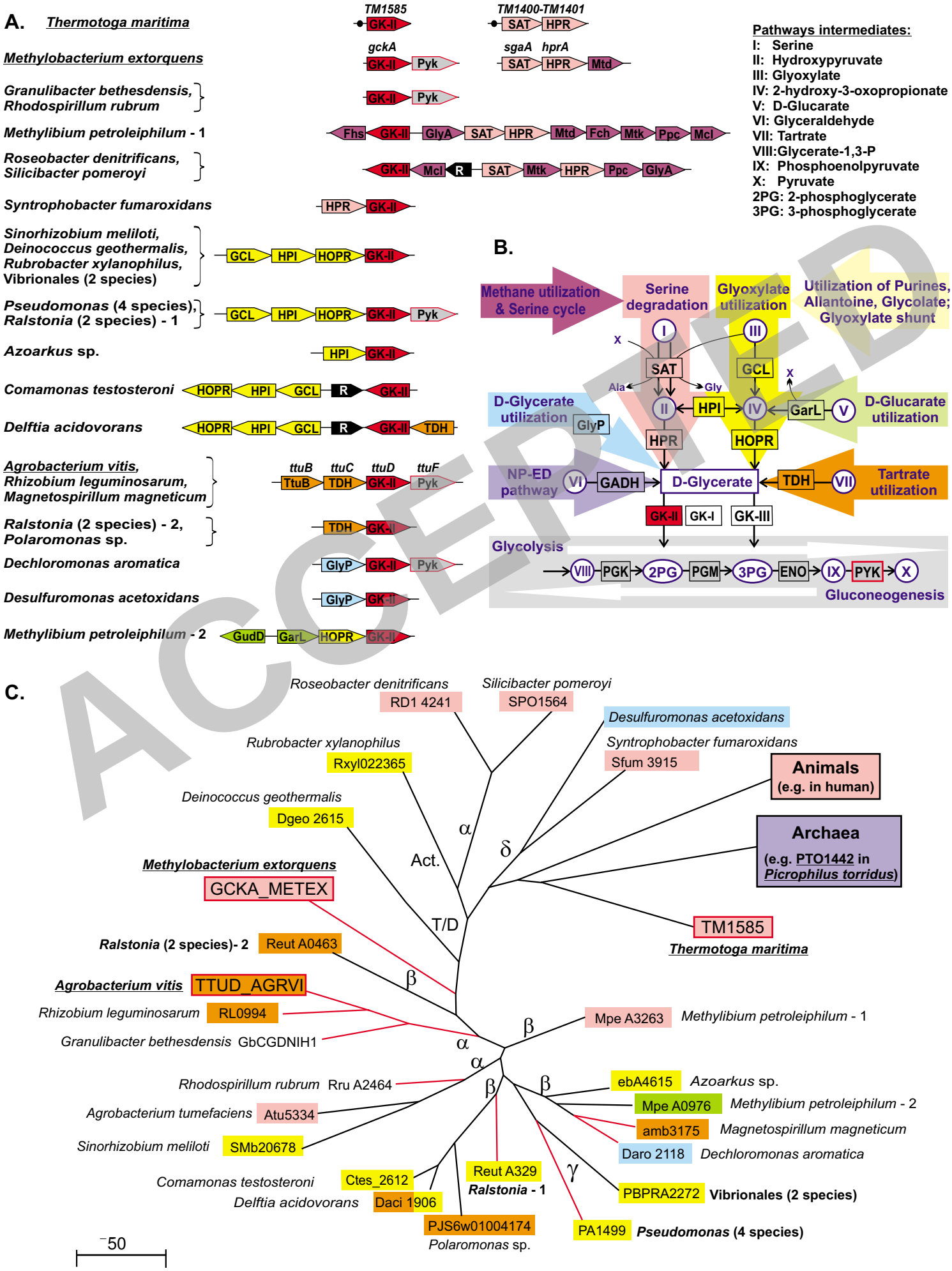

Figure 2.

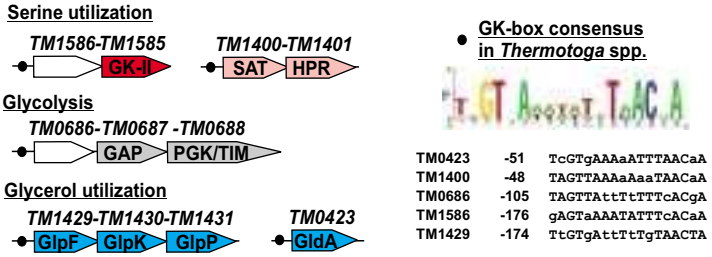

- **GK-box consensus in *Thermotoga* spp.**

TM0423	-51	TcGTgAAAaATTTAACaA
TM1400	-48	TAGTTAAAaAaaTAACaA
TM0686	-105	TAGTTAttTtTTTcACgA
TM1586	-176	gAGTaAAATATTTcACaA
TM1429	-174	TtGTgAttTtTgTAACTA

Figure 3.